Surface solitary waves propagating in a stratified fluid

Masoud Hayatdavoodi[a,b], Tianyu Zhang[a], Binbin Zhao[a] and R. Cengiz Ertekin[a,c]
a. College of Shipbuilding Engineering, Harbin Engineering University, Harbin, China
b. School of Science and Engineering, University of Dundee, Dundee DD1 4HN, UK
c. Department of Ocean & Resources Engineering, University of Hawaii, HI 96822, USA
Email: mhayatdavoodi@dundee.ac.uk

Introduction

In oceans, variations in water density with depth lead to fluid stratification, which, together with strong tidal currents and uneven topography, generates internal waves, often manifesting as shoreward-propagating solitary waves, which are widespread, particularly in coastal regions (see e.g., Garrett & Munk (1979)). In natural ocean settings, surface waves, internal waves, and currents coexist. Observations demonstrate that internal waves can strongly influence surface waves by modifying their wavelength, height, and symmetry, inducing surface-wave focusing, and in some cases triggering wave breaking, see e.g. Gargett & Hughes (1972), Lewis et al. (1974), Magalhães et al. (2021). Localised multi-layer fluid systems (such as oil slicks or sludge layers in coastal zones, harbours, and channels) can similarly modify wave mechanics, see e.g. Kashiwagi (2007). Interactions between surface and internal waves (and currents in general) is a nonlinear process and the resulting dynamics cannot be described with a linear superposition of these. Also these interactions influence hydrodynamic loads and structural responses. This is especially critical for offshore wind turbine foundations, whether fixed or floating, that typically involve cylindrical elements extending vertically through fluid layers exposed to combined surface and internal waves. A comprehensive analysis, therefore, requires consideration of coupled surface-internal wave interactions and their combined influence on structural behaviour.

Nearly all existing research examines surface waves without stratification and internal waves, or internal waves without surface-wave presence (via the rigid-lid approximation, e.g., by Camassa et al. (2006)), and when the free surface is included, surface-wave motion is typically neglected (e.g., Kodaira et al. (2016)). There is a clear gap in understanding how surface and internal waves interact, leading to an incomplete representation of real ocean environments, particularly in places where stratified fluid and internal waves are present. One forbidding challenge in simultaneously considering surface and internal waves is the inherent scale differences in motions and wave dynamics, and models are designed for one or the other, determined by the relevant physics, but not both. This research aims to fill this gap in studying the interactions between surface waves and internal waves.

Two primary mechanisms influence surface-wave dynamics in stratified fluids: (i) modifications to surface-wave dynamics due to the presence of stratification, and (ii) the direct impact of coexisting surface-internal waves. This abstract is concerned with mechanism (i), namely the assessment of surface waves propagating in a stratified fluid and the quantification of the effects of fluid stratification on wave dynamics.

The Green-Naghdi Governing Equations

We consider the propagation of waves in a stratified fluid consisting of two layers of inviscid and incompressible fluids. The upper fluid layer (with properties specified by subscript I in Fig. 1) is bounded by the free surface above and the lower fluid layer below. The lower layer (specified by subscript II) is bounded above by Fluid I and below by a stationary seafloor. We assume a sharp interface (i.e. a thin pycnocline) and the absence of mixing or gaps between the two fluid layers over time, such that the solutions in different layers are directly connected at the interfaces. The two fluid layers may have arbitrary but finite thicknesses. The fluids experience gravitational acceleration g in the negative z direction in a Cartesian coordinate system.

We employ the Green-Naghdi (GN) equations (Green & Naghdi (1976*a*,*b*)) to study this problem.

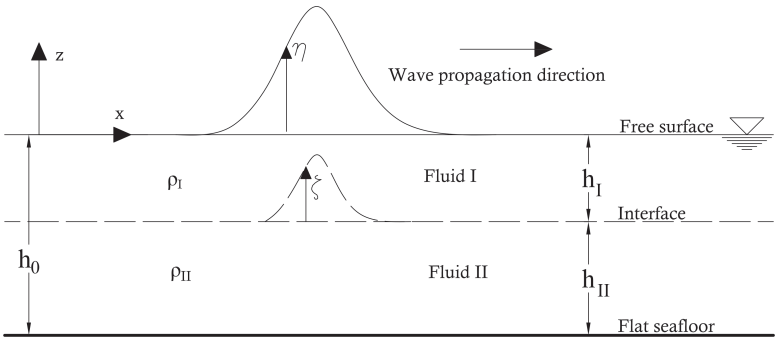

Figure 1: Schematic of a solitary surface wave propagating in a two-layer fluid system. η and ζ are measured from the SWL and the fluids' interface, respectively.

GN equations are derived from Euler's equations, given as

$$\frac{\partial u_i}{\partial x} + \frac{\partial w_i}{\partial z} = 0, \tag{1}$$

$$\frac{\partial u_i}{\partial t} + u_i\frac{\partial u_i}{\partial x} + w_i\frac{\partial u_i}{\partial z} = -\frac{1}{\rho_i}\frac{\partial p_i}{\partial x}, \tag{2}$$

$$\frac{\partial w_i}{\partial t} + u_i\frac{\partial w_i}{\partial x} + w_i\frac{\partial w_i}{\partial z} = -\frac{1}{\rho_i}\frac{\partial p_i}{\partial z} - g, \tag{3}$$

where u and w denote the horizontal and vertical velocity components, respectively, p is the pressure, ρ is the fluid density, and t is time. Throughout this paper, the subscript i takes the values $i = I, II$ and denotes the fluid layer. GN theory simplifies Euler's equations by prescribing the form of the velocity field across the fluid column, here approximated by polynomial functions as (see e.g. Zhao et al. (2020))

$$u_i(x,z,t) = \sum_{n=0}^{K_i} u_{n,i}(x,t)z^n, \qquad w_i(x,z,t) = \sum_{n=0}^{K_i} w_{n,i}(x,t)z^n, \tag{4}$$

where $u_{n,i}$ and $w_{n,i}$ are the unknown horizontal and vertical velocity coefficients in the polynomial expansion. GN theory forms a hierarchy of equations, organised into different levels defined by the upper summation limit $K \geq 1$. In this study, K_I and K_{II} are defined independently for each layer, and we use the notation GN-K_I-K_{II} to specify the level of the theory adopted for the upper and lower layers, respectively.

To obtain the final form of the governing equations, the prescribed velocity profiles are substituted into Euler's equations, subject to exact kinematic and dynamic boundary conditions at the free surface η (measured from the still-water level, SWL), the time-dependent interface between the two fluids ζ (measured from the initial position of the interface, at $-h_I$ from the SWL), and the stationary seafloor at the bottom ($z = -h$):

$$w_I = \frac{\partial \eta}{\partial t} + u_I\frac{\partial \eta}{\partial x} \qquad \text{at} \qquad z = \eta(x,t), \tag{5}$$

$$w_i = \frac{\partial \zeta}{\partial t} + u_i\frac{\partial \zeta}{\partial x} \qquad \text{at} \qquad z = \zeta(x,t) - h_I, \tag{6}$$

$$w_{II} = 0 \qquad \text{at} \qquad z = -h_0, \tag{7}$$

$$\hat{p}_I = \hat{p}_{atm} \qquad \text{at} \qquad z = \eta(x,t), \tag{8}$$

$$\bar{p}_I = \hat{p}_{II} \qquad \text{at} \qquad z = \zeta(x,t) - h_I, \tag{9}$$

where $\bar{p}$ and $\hat{p}$ denote the bottom and top pressures of a given fluid layer (as specified by the subscripts), and $\hat{p}_{\text{atm}}$ is the atmospheric pressure above the upper fluid layer, taken to be zero here. Further details of the derivation of the GN equations used in this study can be found in Zhao et al. (2024).

The equations are solved numerically using a five-point central-difference method for spatial derivations, and a fourth-order predictor-corrector Adams-Bashforth-Moulton scheme for time marching. See Zhao et al. (2020) for further details about the numerical solution of the GN model.

Results and Discussion

A two-dimensional stratified fluid domain, consisting of two fluid layers (Fluid I above and Fluid II below) of arbitrary thicknesses and densities is considered. In this study, we confine attention to the

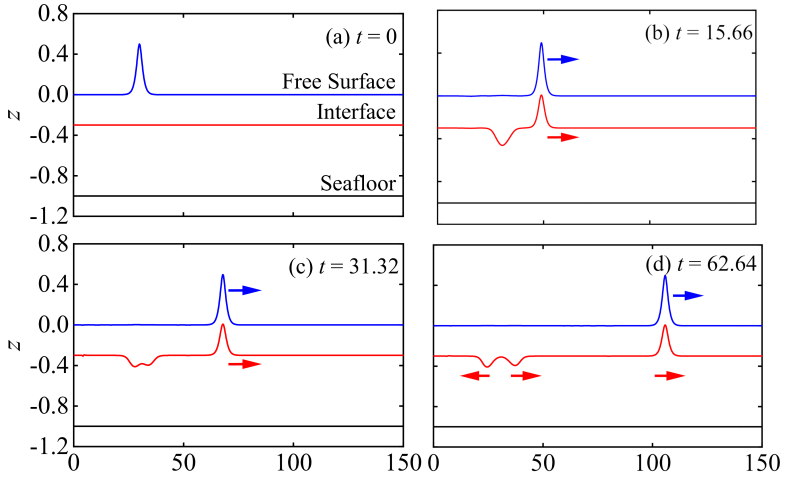

Figure 2: Snapshots of the surface elevation (blue) and the interface between the two fluids (red), $\bar{h} = 0.3/0.7$. Also shown are the propagation direction of the surface wave, the induced internal solitary wave propagating under the surface wave, and the negative humps which propagate in opposite directions at a significantly slower speed.

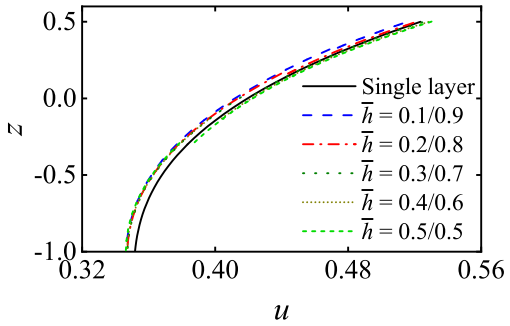

Figure 3: Snapshot of horizontal velocity distribution across the water depth under the wave crest at time $t = 31.32$ for variable $\bar{h}$ ratios, including the case of a homogenous fluid. In all stratified fluid cases, there is a clear jump in horizontal velocity distribution across the interface of the two fluids.

propagation of surface solitary waves over a flat seafloor, shown schematically in Fig. 1, together with the Cartesian coordinate system used. The GN solitary wave is generated at time $t = 0$ by an external excitation force, which is removed for $t > 0$. In this study, $\rho_I = 995\,\mathrm{kg/m^3}$ and $\rho_{II} = 1035\,\mathrm{kg/m^3}$ are used and remain invariant in all cases. GN-4-4 is found to be the converged level of the equations and is therefore used throughout. Results are presented in dimensionless form using ρ_I, g, and h_0 as a dimensionally independent set. Keeping the total water depth (h_0) fixed, the study is performed for various ratios of the upper- to lower-layer thicknesses, $\bar{h} = h_I/h_{II}$. For comparison, we also consider wave propagation in a homogenous (single-layer) fluid with density ρ_I. The solitary wave amplitude is fixed at $A = 0.5$, and at $t = 0$, the solitary wave peak is at $x = 30$.

Figure 2 presents snapshots of the fluid domain at three times, namely $t = 0$ (corresponding to the initial condition), $t = 31.32$, and $t = 62.64$, for the case $\bar{h} = 0.3/0.7$, showing both the free surface and the interface between the two fluids. It is observed that the surface solitary wave induces the formation of an internal wave in the form of a negative hump at the interface, as well as a down-wave-propagating positive internal solitary wave beneath the crest of the surface solitary wave. While the down-wave-propagating positive internal solitary wave appears stable and travels at the same speed as the surface wave, the negative hump undergoes a soliton fission process and separates into two components, one propagating up-wave and the other down-wave. Although solitary wave is stable, the initial negative-hump internal wave is generated due to instability in the stratified, multi-layer fluid domain.

Figure 3 shows snapshots of the horizontal velocity distribution beneath the solitary-wave crest for different values of $\bar{h}$. These distributions are compared with those of a solitary wave propagating in a homogeneous (single-layer) fluid. In the upper layer (Fluid I), the velocity distribution deviates slightly from the homogeneous-fluid case, with differences becoming more pronounced for smaller $\bar{h}$ values, corresponding to a thinner upper layer. In contrast, the horizontal velocity distribution in Fluid II, while clearly different from the homogeneous-fluid case, remains essentially invariant with respect to the layer thickness ratio.

Figure 4 presents time series of the surface elevation and the interface displacement recorded by a down-wave gauge fixed at $X = 130$. An additional gauge is placed up-wave at $X = 25$ to record the negative hump internal wave. Results are shown for a range of $\bar{h}$ values and, for the surface elevation, are also compared with the corresponding single-layer case. The presence of stratification is observed to affect both the amplitude and the propagation speed of the surface solitary wave. While the surface-

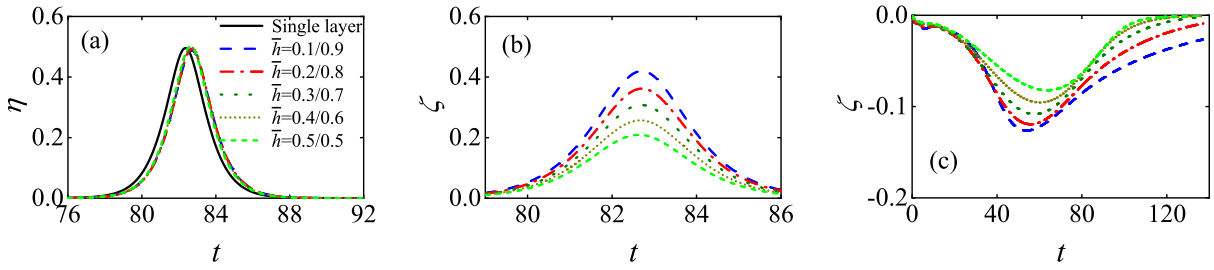

Figure 4: Time series of (a) surface elevation (η) of the surface waves and interface displacement (ζ), showing the (b) positive and (c) negative internal waves for variable $\bar{h}$ ratios.

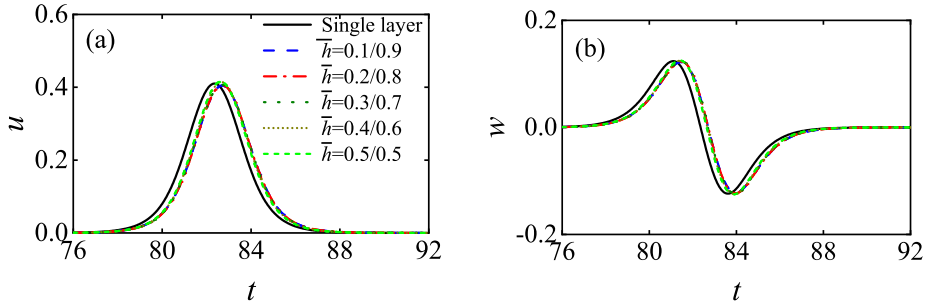

Figure 5: Time series of (a) horizontal (u) and (b) vertical (w) velocities recorded at $z = -0.05$ within the upper fluid layer, for variable $\bar{h}$ ratios.

wave amplitude varies nonlinearly with the layer-thickness ratio, the wave speed is reduced in all two-layer cases. Figure 4 also reveals remarkable differences in the form and magnitude of the positive internal wave generated by the surface solitary wave. Larger internal-wave peaks occur for smaller values of $\bar{h}$, corresponding to a thinner upper layer. The down-wave-propagating positive internal wave appears stable, whereas the up-wave-going negative hump wave exhibits clear asymmetry.

Time series of the horizontal velocity recorded at $z = -0.05$ for a range of $\bar{h}$ values are shown in Fig. 5 and compared with the corresponding single-layer results. Near the free surface, the peak horizontal velocities in the stratified cases differ slightly from those in the single-layer case, with largest differences appearing for smaller $\bar{h}$. The vertical velocities near the free surface appear largely insensitive to variations in the layer-thickness ratio, although the wave propagation speed is clearly reduced.

References

Camassa, R., Choi, W., Michallet, H., Rusås, P. O. & Sveen, J. K. (2006), 'On the realm of validity of strongly nonlinear asymptotic approximations for internal waves', *Journal of Fluid Mechanics* **549**, 1–23.

Gargett, A. E. & Hughes, B. A. (1972), 'On the interaction of surface and internal waves', *Journal of Fluid Mechanics* **52**(1), 179–191.

Garrett, C. & Munk, W. (1979), 'Internal waves in the ocean', *Annual Review of Fluid Mechanics* **11**(1), 339–369.

Green, A. E. & Naghdi, P. M. (1976*a*), 'A derivation of equations for wave propagation in water of variable depth', *Journal of Fluid Mechanics* **78**(2), 237–246.

Green, A. E. & Naghdi, P. M. (1976*b*), 'Directed fluid sheets', *Proceedings of the Royal Society of London A* **347**(1651), 447–473.

Kashiwagi, M. (2007), 'Wave drift force in a two-layer fluid of finite depth', *Journal of Engineering Mathematics* **58**, 51–66.

Kodaira, T., Waseda, T., Miyata, M. & Choi, W. (2016), 'Internal solitary waves in a two-fluid system with a free surface', *Journal of Fluid Mechanics* **804**, 201–223.

Lewis, J. E., Lake, B. M. & Ko, D. R. S. (1974), 'On the interaction of internal waves and surface gravity waves', *Journal of Fluid Mechanics* **63**(4), 773–800.

Magalhães, J. M., Alpers, W., Santos-Ferreira, A. M. & Da Silva, J. C. (2021), 'Surface wave breaking caused by internal solitary waves', *Oceanography* **34**(2), 166–176.

Zhao, B., Wang, Z., Duan, W., Ertekin, R. C., Hayatdavoodi, M. & Zhang, T. (2020), 'Experimental and numerical studies on internal solitary waves with a free surface', *Journal of Fluid Mechanics* **899**, A17.

Zhao, B., Zhang, T., Wang, Z., Hayatdavoodi, M., Gou, Y., Ertekin, R. C. & Duan, W. (2024), 'High-level Green–Naghdi model for large-amplitude internal waves in deep water', *Journal of Fluid Mechanics* **988**, A32.